

Time evolution of pulsar obliquity angle from 3D simulations of magnetospheres

Alexander Philippov^{1*}, Alexander Tchekhovskoy^{2,3,4†}, Jason G. Li¹

¹*Department of Astrophysical Sciences, Peyton Hall, Princeton University, Princeton, NJ 08544, USA*

²*Lawrence Berkeley National Laboratory, 1 Cyclotron Rd, Berkeley, CA 94720, USA*

³*University of California Berkeley, Berkeley, CA 94720-3411*

⁴*Formerly at the Center for Theoretical Science, Jadwin Hall, Princeton University, Princeton, NJ 08544, USA; Center for Theoretical Science Fellow*

Accepted . Received ; in original form

ABSTRACT

Isolated pulsars lose their rotational energy due to magnetospheric torques. In addition to merely slowing down pulsar rotation, these torques reorient pulsar magnetic axis and cause the obliquity angle α between the magnetic and rotational axes to evolve in time. Despite actual pulsar magnetospheres are plasma-filled, the time evolution of α has mostly been studied for vacuum pulsar magnetospheres. In this work, we for the first time self-consistently account for the plasma effects by analyzing the results of time-dependent 3D force-free and magnetohydrodynamic (MHD) simulations of pulsar magnetospheres. On general symmetry grounds we show that if a neutron star is spherically symmetric and is embedded with a dipolar magnetic moment, the pulsar evolves such as to minimize its spindown luminosity. Thus, both vacuum and plasma-filled pulsars inevitably evolve toward the aligned configuration ($\alpha = 0$). However, we find that they approach the alignment in qualitatively different ways. Vacuum pulsars come into alignment exponentially fast, $\alpha \propto \exp(-t/\tau)$, with $\tau \sim$ spindown timescale. In contrast, plasma-filled pulsars align much more slowly, according to a power-law in time, $\alpha \propto (t/\tau)^{-1/2}$. We argue that the slow time-evolution of obliquity we find for plasma-filled pulsars can potentially resolve several observational puzzles. We derive the expressions for the alignment torque and timescale and present the time evolution of the pulsar period and obliquity angle. We also derive approximate analytical formulae that describe the numerical results well. Finally, we discuss the astrophysical consequences for pulsar population synthesis and the ramifications for the distribution of pulsar obliquity angles.

Key words: pulsars - neutron stars - magnetospheres

1 INTRODUCTION

Rotation powered pulsars slow down as magnetized winds carry away pulsars' rotational energy. Despite pulsar magnetospheres are filled with plasma (Goldreich & Julian 1969) that produces observed radio emission (see, e.g., Lyne & Graham-Smith 1998; Lyubarsky 2008; Beskin & Philippov 2012 and references therein), most of the early work on understanding the time evolution of pulsars was carried out ignoring plasma effects, i.e., assuming a vacuum magnetosphere, primarily because a quantitative analytic solution was readily available (Deutsch 1955; Goldreich 1970). In this solution, in addition to merely slowing down the star, magnetospheric torques also lead to the alignment of pulsar magnetic and rotational axes. In fact, this alignment process is so efficient that vacuum pulsars become aligned before they have a chance to substantially spin down (Michel & Goldwire 1970). Presently, in the

absence of a self-consistent model, the evolution of pulsar obliquity with time is usually neglected or considered in the framework of the vacuum model that neglects plasma effects in the pulsar magnetosphere (Faucher-Giguère & Kaspi 2006).

Recent advances in axisymmetric (Contopoulos, Kazanas & Fendt 1999; Gruzinov 2005; McKinney 2006; Timokhin 2006) and oblique (Spitkovsky 2006; Kalapotharakos & Contopoulos 2009; Pétri 2012; Li, Spitkovsky & Tchekhovskoy 2012; Kalapotharakos, Contopoulos & Kazanas 2012) force-free and magnetohydrodynamic (MHD) (Komissarov 2006; Tchekhovskoy, Spitkovsky & Li 2013) modeling of pulsar magnetospheres now allow one to self-consistently account for plasma charges and currents that substantially modify the magnetospheric structure and spin-down torques. In this paper we show that the presence of plasma in the magnetosphere also substantially affects the process of pulsar alignment. We start with describing our numerical models in §2 and derive pulsar evolutionary equations in §3. We then calculate the torques and evolution of pulsar obliquity angle in our vacuum magnetospheres in §4 and plasma-filled magnetospheres in §5. We derive

* sashaph@princeton.edu

† Einstein Fellow

Table 1. Model details: model name, pulsar obliquity angle (α), simulation resolution and the radius of the NS, R_* , in units of the light cylinder radius, R_{LC} .

Name	$\alpha[^\circ]$	Resolution*	R_*/R_{LC}
Relativistic MHD models (with HARM):			
HR01A0	0	$128 \times 128 \times 64$	0.1
HR01A45	45	$288 \times 128 \times 256$	0.1
HR01A90	90	$288 \times 128 \times 256$	0.1
HR02A0	0	$256 \times 128 \times 1$	0.2
HR02A15	15	$256 \times 128 \times 128$	0.2
HR02A30	30	$256 \times 128 \times 128$	0.2
HR02A45	45	$256 \times 128 \times 128$	0.2
HR02A60	60	$256 \times 128 \times 128$	0.2
HR02A75	75	$256 \times 128 \times 128$	0.2
HR02A90	90	$256 \times 128 \times 128$	0.2
HR0375A30	30	$256 \times 128 \times 128$	0.375
HR0375A60	60	$256 \times 128 \times 128$	0.375
HR0375A90	90	$256 \times 128 \times 128$	0.375
HR05A30	30	$256 \times 128 \times 128$	0.5
HR05A60	60	$256 \times 128 \times 128$	0.5
HR05A90	90	$256 \times 128 \times 128$	0.5
Force-free models (with AS):†			
ASFF0375A0	0	$1000 \times 1000 \times 1000$	0.375
ASFF0375A15	15	$1000 \times 1000 \times 1000$	0.375
ASFF0375A30	30	$1000 \times 1000 \times 1000$	0.375
ASFF0375A45	45	$1000 \times 1000 \times 1000$	0.375
ASFF0375A60	60	$1000 \times 1000 \times 1000$	0.375
ASFF0375A75	75	$1000 \times 1000 \times 1000$	0.375
ASFF0375A90	90	$1000 \times 1000 \times 1000$	0.375
Vacuum models (with AS):‡			
ASVAC0375A0	0	$1000 \times 1000 \times 1000$	0.375
ASVAC0375A15	15	$1000 \times 1000 \times 1000$	0.375
ASVAC0375A30	30	$1000 \times 1000 \times 1000$	0.375
ASVAC0375A45	45	$1000 \times 1000 \times 1000$	0.375
ASVAC0375A60	60	$1000 \times 1000 \times 1000$	0.375
ASVAC0375A60ext	60	$1000 \times 1000 \times 1000$	0.375
ASVAC0375A75	75	$1000 \times 1000 \times 1000$	0.375
ASVAC0375A90	90	$1000 \times 1000 \times 1000$	0.375

* Given as $N_r \times N_\theta \times N_\phi$ for MHD and $N_x \times N_y \times N_z$ for vacuum and force-free models.

† In all vacuum and force-free models the stellar radius is resolved with 30 cells, with the exception of ASVAC0375A60ext, in which it is resolved with 15 cells.

the relationship between spin-down and alignment torques in §6 and conclude in §7.

2 NUMERICAL METHODS AND PROBLEM SETUP

We carried out a number of time-dependent 3D simulations of oblique pulsar magnetospheres in the relativistic MHD, force-free and vacuum approximations. The models start with a perfectly conducting star of radius R_* that rotates at an angular frequency $\Omega = 2\pi/P$, where P is the pulsar period. The star is embedded with a magnetic dipole field of dipole moment μ that makes an angle α with the rotational axis, Ω . The models are listed in Table 1 and cover the full range of obliquity angles, $\alpha = 0^\circ - 90^\circ$, and a range of angular frequencies, $\Omega R_*/c \equiv R_*/R_{LC} = 0.1 - 0.5$, where $R_{LC} = c/\Omega$ is the light cylinder (LC) radius. We note that the rotation of the star causes substantial deviations away from the initial dipolar magnetic field, especially around and beyond the LC where special relativistic effects become important (Bai & Spitkovsky 2010a,b).

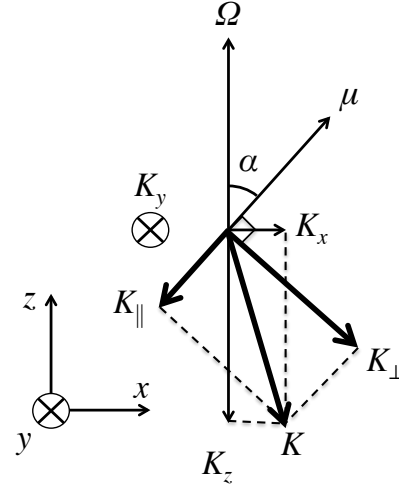


Figure 1. Coordinate system used in this paper. Vector Ω shows the pulsar rotational axis, μ the magnetic axis, and K the magnetospheric torque on the NS. The z -component of the torque, K_z , acts opposite to Ω , therefore it decreases the magnitude of Ω without changing its direction, whereas K_x and K_y components act perpendicular to Ω . Therefore, while they keep the magnitude of Ω the same, they change its orientation relative to μ . See §3 for more detail. Description of K_{\parallel} and K_{\perp} is given in Section 6.

We carry out our relativistic MHD simulations (Tab. 1) using the HARM code (Gammie et al. 2003; Tchekhovskoy et al. 2007; McKinney & Blandford 2009; Tchekhovskoy et al. 2011; McKinney et al. 2012) in a spherical polar grid, r, θ, φ , but we sometimes also use the cylindrical radius, $R = r \sin \theta$. We denote these models as HRmmAnn, where mm represents the value of R_*/R_{LC} and nn the value of α in degrees. We carry out our force-free and vacuum simulations (Tab. 1) with the code by Spitkovsky (2006) in a Cartesian grid and denote the force-free models as ASFFnnAmm and vacuum models as ASVACnnAmm. More details of the setup and general properties of our models are described in Tchekhovskoy et al. (2013) for relativistic MHD models and in Spitkovsky (2006); Li et al. (2012) for force-free and vacuum models.

3 TORQUES AND THEIR EFFECT ON PULSAR OBLIQUITY

To compute the torques acting on the neutron star (NS), we choose an inertial coordinate system illustrated in Figure 1: (e_x, e_y, e_z) , with the magnetic moment μ instantaneously lying in the x - z plane and Ω instantaneously pointing along the z -axis: $e_x = [(e_\Omega \times e_\mu) \times e_\Omega]$, $e_y = [e_\Omega \times e_\mu]$, and $e_z = e_\Omega$. The i -th component ($i = x, y, z$) of the torque acting on the star is given by (Landau & Lifshitz 1960)

$$K_i = - \int \varepsilon_{ijk} r_j T_{kl} dA_l, \quad (1)$$

where the integral is carried over the entire surface area of the NS, summation over repeated indices is implied, ε_{ijk} is the antisymmetric tensor, $r = (x, y, z)$, dA_l is the element of the surface area normal to r_l , and T_{kl} are the physical components of energy-momentum tensor. The minus sign in eq. (1) appears because the angular momentum carried by the outgoing wind is of the opposite sign to the rate of change of the angular momentum of the NS. In spherical coordinates, in which we carried out our relativistic MHD models,

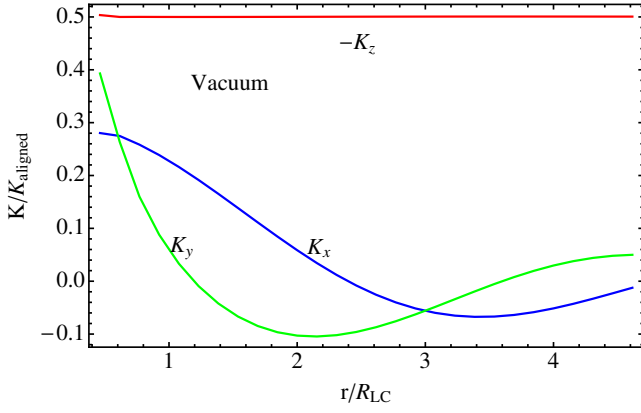


Figure 2. Radial dependence of torque components K_x , K_y and K_z calculated using the components of energy-momentum tensor in simulation AS-VAC0375A60ext. The z -component of the magnetospheric torque, K_z , is conserved and independent of the distance from the star, so it can be measured at any distance. The two other components of the torque, K_x and K_y , show significant variations with radius and should be measured at the surface of the star, where the torque is transferred to the NS crust.

eq. (1) becomes (Michel & Goldwire 1970):

$$K_x = \int r(T_{r\theta} \sin \varphi + T_{r\varphi} \cos \theta \cos \varphi) dA, \quad (2a)$$

$$K_y = - \int r(T_{r\theta} \cos \varphi - T_{r\varphi} \cos \theta \sin \varphi) dA, \quad (2b)$$

$$K_z = - \int r(T_{r\varphi} \sin \theta) dA. \quad (2c)$$

The evolution equations for the angular velocity of the pulsar are:

$$I \frac{d\Omega}{dt} = K, \quad (3)$$

where I is the stellar moment of inertia.¹ The z -component of the torque, K_z , acts opposite to $\Omega \equiv \Omega e_z$, therefore it decreases the magnitude of Ω without changing its direction:

$$I \frac{d\Omega}{dt} = K_z. \quad (4)$$

In contrast, K_x and K_y components act perpendicular to Ω (see Fig. 1). Therefore, while they keep the magnitude of Ω the same, they change its orientation relative to μ .

In particular, K_x , causes Ω to rotate clock-wise in the μ - Ω plane (see Fig. 1),

$$I\Omega \frac{d\alpha}{dt} = -K_x, \quad (5)$$

where we used $d\Omega_x/dt = -\Omega d\alpha/dt$ for clock-wise rotation of Ω in μ - Ω plane. While it is tempting conclude that this causes the direction of rotational axis to evolve, this is not so. This is because while the vector Ω rotates in μ - Ω plane as described above, this plane itself rotates about e_z together with the NS. If one averages over this rapid rotation of the NS it is easy to see that the direction of Ω remains unchanged as seen by a stationary observer, and it is the direction of μ that is changing according to eq. (5).

¹ For simplicity, we assume spherical symmetry of the star, e.g., we neglect possible effects of stellar oblateness caused by its rapid rotation. Non-sphericity of the NS can lead to non-trivial effects, which were carefully studied by Melatos (2000) within a vacuum framework. We defer the analysis of similar effects within an MHD framework to future work.

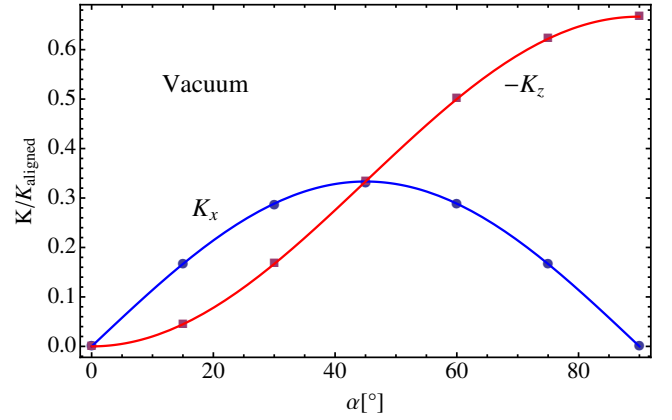


Figure 3. The dependence of spindown torque K_z (red squares) and alignment torque K_x (blue circles) on pulsar obliquity angle α in vacuum models (see Tab. 1). Solid lines show the analytic expressions (7)-(8), whereas dots and squares show our numerical results (models ASVAC0375A0–ASVAC037590). The agreement of the numerical results with the analytical expressions is excellent.

Analogously, K_y -component causes Ω to rotate out of μ - Ω plane. As a result, the tip of the vector Ω traces out a circle on the surface of the NS (this circle is centered at the magnetic pole) and does so at an angular frequency Ω_{prec} given by

$$I\Omega\Omega_{\text{prec}} = -\frac{K_y}{\sin \alpha}, \quad (6)$$

where we used $d\Omega_y/dt = -\Omega\Omega_{\text{prec}}$ for rotation of Ω out of the μ - Ω plane. As we neglect stellar non-sphericity (see footnote 1), eqs. (4) and (5) are decoupled from eq. (6) and can be solved for independently. We do so in §4 for vacuum and in §5 for force-free and MHD magnetospheres.

4 VACUUM PULSAR MAGNETOSPHERES

Using an exact solution for the magnetospheric structure in vacuum (Deutsch 1955), it is straightforward to compute the surface magnetospheric torque (eq. 1) on the NS (Michel & Goldwire 1970):

$$K_x = \frac{2}{3} K_{\text{aligned}} \sin \alpha \cos \alpha, \quad (7)$$

$$K_z = -\frac{2}{3} K_{\text{aligned}} \sin^2 \alpha, \quad (8)$$

where, as we discuss in §5,

$$K_{\text{aligned}} = \frac{\mu^2 \Omega^3}{c^3} \quad (9)$$

is the spin-down torque of an aligned force-free or MHD pulsar.

As a comparison to the analytic model, we carried out numerical vacuum magnetosphere simulations for a wide range of obliquity values (models ASVACxxx, see Tab. 1). For instance, Fig. 2 shows the radial run of the components of K , which we computed according to eq. (1), for our fiducial vacuum model VAC0375A60ext, which is a simulation with an obliquity angle $\alpha = 60^\circ$ and the period such that $R_*/R_{\text{LC}} = 0.375$. As expected, the z -component of the magnetospheric torque, K_z , is conserved and independent of the distance from the star (this is a manifestation of the conservation of the z -component of angular momentum). For this reason, the value of K_z can be measured at essentially any distance from the star: e.g., $K_z \approx -0.5$ in this simulation, as can be

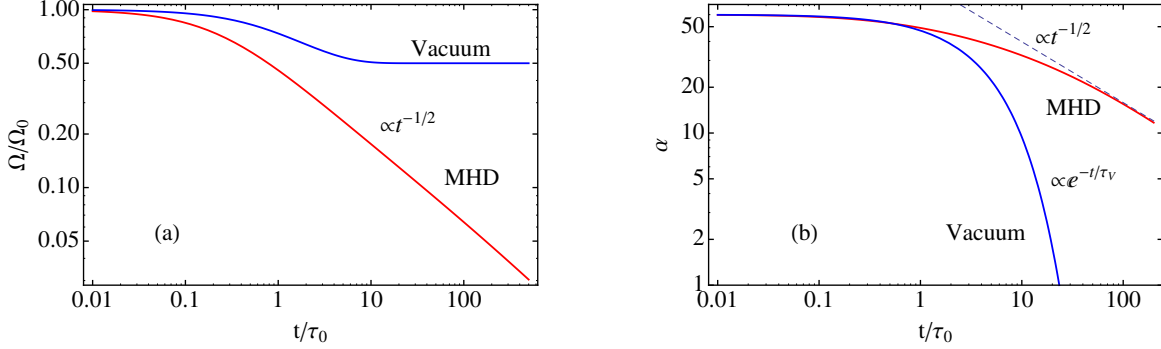


Figure 4. [Left panel]: The time evolution of pulsar angular frequency, Ω , for an initial obliquity angle $\alpha_0 = 60^\circ$ and an initial period $P_0 = 10$ ms for vacuum (blue curve) and MHD (red curve) pulsars. While vacuum pulsars settle to a constant rotation rate $\Omega_\infty = \Omega_0 \cos \alpha_0 = \Omega_0/2$ on a timescale that is of order of pulsar spindown time τ_0 , plasma-filled (MHD) pulsars continue to spin down as a power-law in time, $\Omega \propto t^{-1/2}$. The continued decrease of Ω in plasma-filled magnetospheres can help to explain the origin of normal pulsars with periods of order of one second (see §5 for a discussion). **[Right panel]:** The time evolution of pulsar obliquity angle for vacuum (blue) and MHD (red) pulsars. Vacuum pulsar evolves exponentially fast to an aligned configuration, while for an MHD pulsar the obliquity angle decreases to zero as a power-law, $\alpha \propto t^{-1/2}$. The dashed line shows the asymptotical behaviour given by equation (17).

seen in Fig. 2. The two other components of the torque, K_x and K_y , show sinusoidal-like variations with radius,² and it is important that we measure these components at the correct location — the stellar surface — at which the magnetospheric torques are transferred to the NS crust.

Since the radial profile of K_x becomes flat at small r/R_{LC} , we can reliably measure its value at the NS surface, $K_x(R_*/R_{LC}) \equiv K_x(\Omega R_*/c)$. This also means that this value is essentially independent of the pulsar period (which sets R_*/R_{LC}): e.g., Fig. 2 shows that $K_x(r/R_{LC} \ll 1) \approx 0.28$. In contrast, K_y approaches small radii at a steep slope (see Fig. 2). This is because $K_y(R_*)$ diverges as $R_*/R_{LC} \rightarrow 0$ (Davis & Goldstein 1970). Due to this, extra care is needed to measure K_y at the stellar surface in numerical models. In this Letter we concentrate on K_x and K_z torque components and do not carry out any K_y measurements.

Figure 3 shows that the analytic expressions for torque components, K_x and K_z , which are given by eqs. (7) and (8), are in excellent agreement with our numerical vacuum results, which are shown with discrete data points in Fig. 3 (models ASVACxxAyy, see Tab. 1). To determine the time evolution of pulsar’s Ω and α , we need to solve the system of eqs. (4) and (5) coupled with the vacuum expressions for the torque, eqs. (7) and (8).

It is easy to show that the quantity,

$$\Omega \cos \alpha = \Omega_0 \cos \alpha_0, \quad (10)$$

is an integral of motion, where the subscript “0” refers to the values of pulsar variables at an initial time, $t = t_0$. One can also obtain the following analytic solution for the time evolution of Ω and α (Michel & Goldwire 1970):

$$\Omega = \Omega_0 \left\{ 1 + \left[1 - \exp\left(-2t/\tau_{\text{align}}^{\text{vac}}\right) \right] \tan^2 \alpha_0 \right\}^{-1/2} \quad (11)$$

$$\sin \alpha = \sin \alpha_0 \exp\left(-t/\tau_{\text{align}}^{\text{vac}}\right), \quad (12)$$

where $\tau_{\text{align}}^{\text{vac}} = 1.5\tau_0 \cos^{-2} \alpha_0$ is the alignment timescale of a vacuum pulsar and $\tau_0 = Ic^3/\mu^2\Omega_0^2$ is the characteristic spindown time of a pulsar.

From eq. (10) it is immediately clear that for pulsar’s rotation to appreciably slow down from its initial value, $\Omega \ll \Omega_0$, one must start with a nearly orthogonal pulsar,

$$\cos \alpha_0 = \frac{\Omega}{\Omega_0} \cos \alpha \leq \frac{\Omega}{\Omega_0} \ll 1. \quad (13)$$

For instance, for a 10-millisecond pulsar to end up as a normal 1-second pulsar, the pulsar must have been born with an extreme obliquity, $\alpha_0 \geq 89.4^\circ$ (see also Michel & Goldwire 1970), which is unlikely if dipole moment orientation is random at birth.

The solid blue line in the left panel of Fig. 4 illustrates that the period of a pulsar of a characteristic initial obliquity (we took $\alpha_0 = 60^\circ$ as an example), can increase in its lifetime by at most a factor of few: its rotational frequency levels off at $\Omega = \Omega_0 \cos \alpha_0 = 0.5\Omega_0$ and obliquity vanishes, $\alpha = 0$, at $t \gtrsim \tau_{\text{align}}^{\text{vac}} = 6\tau_0$ (see eqs. 11–12; the numerical evaluation was performed for $\alpha_0 = 60^\circ$), in agreement with the blue curve in the left panel of Fig. 4. Therefore, if most pulsars start out as rapid rotators (with periods of few to tens of milliseconds) with a random orientation of their magnetic dipole moment, it is difficult to reconcile the observed abundance of normal pulsars (with periods of seconds) and the paucity of such pulsars expected in the vacuum approximation.

Goldreich (1970) found that such a rapid evolution of pulsar obliquity toward alignment does not occur if stellar non-sphericity is taken into account, which makes it easier to reconcile the expected pulsar period distribution with the observed one. However, this and other studies (e.g., Michel & Goldwire 1970; Melatos 2000) on pulsar alignment rely on the vacuum approximation to describe pulsar magnetospheres. This is a rough description of magnetospheres in nature because it neglects all plasma effects, in particular charges and currents, that play a major role in shaping the magnetospheric structure (e.g., Spitkovsky 2006). How does pulsar obliquity evolution change once plasma effects are accounted for?

5 PLASMA-FILLED PULSAR MAGNETOSPHERES

In this section we compute magnetospheric torques and pulsar obliquity evolution while accounting for the plasma effects on the

² These variations are an imprint of the periodic angular structure of an oblique magnetosphere that is carried out by the magnetospheric outflow.

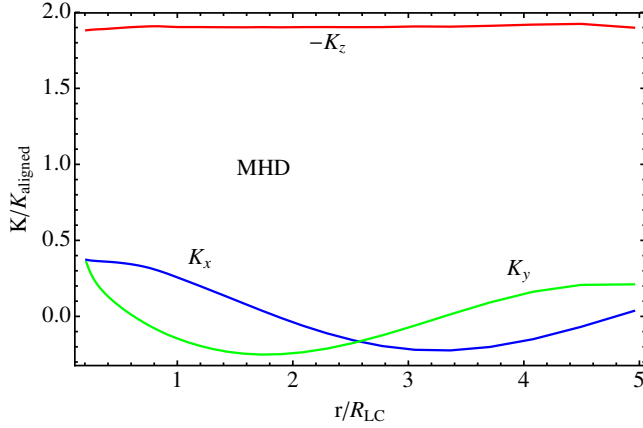


Figure 5. The radial profile of torque components K_x , K_y and K_z calculated using the components of energy-momentum tensor in our fiducial MHD simulation HR02A60. Similarly to the vacuum case (Fig. 2), the z -component of the magnetospheric torque, K_z , is conserved and independent of the distance from the star, so it can be measured at any distance. The two other components of the torque, K_x and K_y , vary with radius, and need to be measured at the surface of the star, where the torques are transferred to the NS crust.

pulsar magnetosphere. In this work, we neglect the effects of the possible non-sphericity of the NS (see footnote 1) and higher order multipole components of the stellar field.

We have carried out a number of relativistic MHD models for a full range of pulsar obliquity, $\alpha = 0-90^\circ$, and a rather wide range of pulsar period, $R_*/R_{LC} = 0.1-0.5$ (models HRxxAyy, see Tab. 1). The results of our force-free models (models ASFFxxAyy in Tab. 1) are similar to MHD and are not shown. Radial dependence for magnetospheric torque components in our fiducial MHD model, HR02A60, which has $\alpha = 60^\circ$ and $R_*/R_{LC} = 0.2$, is shown in Fig. 5.

The comparison to our fiducial vacuum model, which is shown in Fig. 2, indicates that there are many qualitative similarities between the two models: K_z is conserved as a function of distance, whereas K_x and K_y show sinusoidal-like variations with distance. Quantitatively, however, several clear differences emerge: we have $K_z \approx -2$ in the MHD case as opposed to $K_z \approx -0.5$ in the vacuum case, a manifestation of a larger spin-down of plasma-filled (force-free and MHD) magnetospheres in comparison to vacuum magnetospheres (Spitkovsky 2006). Due to this, the relative importance of the alignment torque, or the ratio $K_x/|K_z|$, is a factor of a few smaller in our fiducial MHD simulation, ≈ 0.2 , than in the vacuum one, ≈ 0.6 . This indicates that the presence of the plasma in the magnetosphere, through the associated charges and currents, suppresses the alignment torque relative to the spin-down torque. Therefore, we might expect that pulsar obliquity angle evolution in plasma-filled magnetosphere case (in MHD and force-free approximations) will be slower than in the vacuum case.

To test this hypothesis, we carried out MHD simulations for a full range of obliquity angles. Figure 6 shows our MHD results for a particular value of pulsar period, $R_*/R_{LC} = 0.2$. They are well-described by the following fits:

$$K_x = k_2 K_{\text{aligned}} \sin \alpha \cos \alpha, \quad (14)$$

$$K_z = -K_{\text{aligned}} (k_0 + k_1 \sin^2 \alpha), \quad (15)$$

where $k_0 \approx k_2 \approx 1$ and $k_1 \approx 1.2$. Interestingly, since $K_x > 0$, MHD pulsars evolve toward alignment, just as their vacuum counterparts.

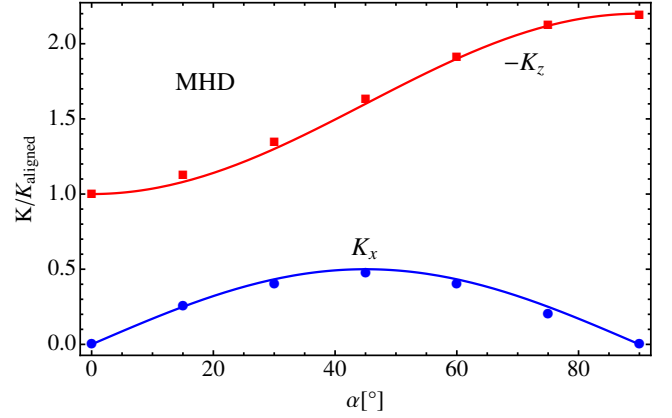


Figure 6. The dependence of spindown torque K_z (red curve) and alignment torque K_x (blue curve) on pulsar obliquity angle α in our MHD models with $R_*/R_{LC} = 0.2$. Solid lines show fitted expressions (14)–(15) with $k_1 \approx 1.2$ and $k_2 \approx 1$, whereas dots and squares show our numerical results (models HR02A0–HR02A90).

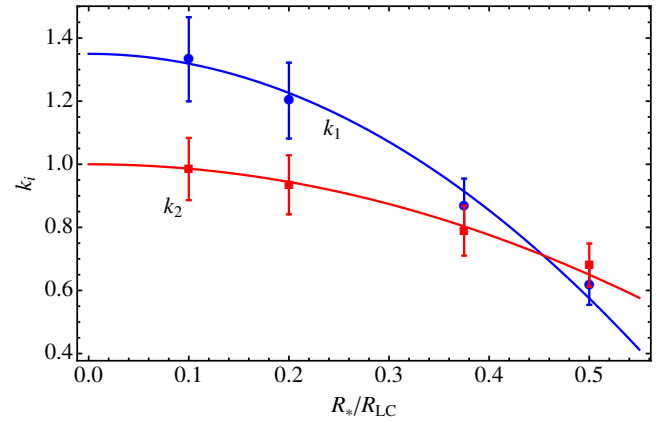


Figure 7. The dependence on the radius of the NS of the coefficients k_1 and k_2 that enter eqs. (14)–(15). To determine their values most accurately, we measured the value of k_1 from the simulations with $\alpha = 90^\circ$ (blue circles) and the value of k_2 from the simulations with $\alpha = 45^\circ$ (red rectangles). Red and blue lines are parabolic fits to the numerical data points. The shown error bars at the level of 10 per cent approximately indicate the uncertainties due to the measurements of the torque on the stellar surface and the differences in the values of k_1 and k_2 obtained in the simulations carried out at different obliquity angles.

As we will see below, however, they approach alignment along very different paths. Note that the system of equations (14)–(15) reduces to that for the vacuum case (eqs. 7–8) for $k_0 = 0$, $k_1 = k_2 = 2/3$.

Figure 7 shows that k_i , $i = 0, 1, 2$, exhibit a weak dependence on R_*/R_{LC} : $k_0 \approx 1$ is virtually independent of R_*/R_{LC} (not shown in Fig. 7) and k_1 and k_2 display a relatively weak dependence on R_*/R_{LC} . Given the symmetry of the problem with respect to the direction of rotation (the sign of Ω), we expect that only even powers of $R_*/R_{LC} \equiv \Omega R_*/c$ enter into the expressions for k_i . However, given the limited range in R_*/R_{LC} accessible to us numerically (the simulations become prohibitively expensive at small values of R_*/R_{LC}), we cannot robustly constrain the complete functional form of k_1 and k_2 as a function of R_*/R_{LC} . We observe a possible indication of parabolic dependence and obtain the following approximations: $k_1 \approx 1.4 - 3.1 \times (R_*/R_{LC})^2$ and $k_2 \approx 1 - 1.4 \times (R_*/R_{LC})^2$.

The origin of this dependence will be studied in future work. However, as deviations from unity are not very large, we will sometimes for convenience neglect this weak spin-dependence of k_1 and k_2 .

We now combine the expressions for torques in the MHD approximation, eqs. (14) and (15), with the evolutionary equations (4) and (5). Under the assumption that factors k_1 and k_2 are constant, we obtain that the quantity,

$$\Omega \left(\frac{\cos^{k_1+1} \alpha}{\sin \alpha} \right)^{1/k_2} = \Omega_0 \left(\frac{\cos^{k_1+1} \alpha_0}{\sin \alpha_0} \right)^{1/k_2}, \quad (16)$$

is conserved in the evolution of a pulsar in both the MHD and force-free approximations. We will see below that eq. (16) imposes less rigidity on pulsar time evolution as compared to the vacuum counterpart, eq. (10).

If we approximately take $k_0 \approx k_1 \approx k_2 \approx 1$, we can derive an analytic solution for the evolution of pulsar obliquity angle, α :

$$\frac{1}{2 \sin^2 \alpha} + \log(\sin \alpha) = \frac{t}{\tau_{\text{align}}^{\text{MHD}}} + \frac{1}{2 \sin^2 \alpha_0} + \log(\sin \alpha_0), \quad (17)$$

where $\tau_{\text{align}}^{\text{MHD}} = \tau_0 \sin^2 \alpha_0 / \cos^4 \alpha_0$ is MHD pulsar alignment timescale.

Figure 4 compares the evolution of Ω and α for an initial obliquity of $\alpha_0 = 60^\circ$ for MHD with k_1 and k_2 shown on Fig. 7 and vacuum models. From Fig. 4(b) it is clear that asymptotically late in time, at $t \gg \tau_{\text{align}}^{\text{MHD}} = 12\tau_0$ (the numerical evaluation is for $\alpha = 60^\circ$), MHD pulsar obliquity decreases as a power-law, $\alpha \propto t^{-1/2}$ (see eq. 17). As this is much slower than in vacuum, where $\alpha \propto \exp(-t/\tau_{\text{align}}^{\text{vac}})$ (see eq. 12), this confirms our expectation that pulsar alignment in MHD magnetospheres occurs at a much slower rate than in vacuum magnetospheres.

As we discussed in §4, a concerning aspect of vacuum pulsars is that their period generally increases only by at most factor of a few and asymptotes to a constant value, $P \approx \text{few} \times P_0$, which is generally too small to be consistent with periods of a few seconds commonly seen in normal pulsars. In contrast, in the MHD approximation pulsar period increases as a power-law, $P \approx P_0(t/\tau_0)^{1/2}$, with virtually no upper limit. This makes it much more comfortable to explain the formation of normal pulsars as initially born as rapidly rotating pulsars with periods of few to tens of millisecond (see §4).

Why do plasma-filled and vacuum pulsars have such different time-evolution? The key difference is in the spin-down rate of an aligned rotator. For instance, since a nearly aligned ($\alpha \ll 1$) vacuum pulsar essentially does not spin down, $\Omega \propto t^0$, due to eqs. (5), (9) and (14), we get $d\alpha/dt \propto \alpha \Omega^3 \propto \alpha t^0$, giving us the exponential decay of the obliquity angle, $\alpha \propto \exp(-t/\tau)$. In contrast, since a nearly aligned ($\alpha \ll 1$) plasma-filled pulsar spins down, $\Omega \propto t^{-1/2}$, we get $d\alpha/dt \propto \alpha \Omega^3 \propto \alpha t^{-3/2}$, thus giving us the power-law evolution, $\alpha \propto (t/\tau)^{-1/2}$.

6 RELATIONSHIP OF SPIN-DOWN AND ALIGNMENT

In this section we present a useful parametrization for torque components that unifies the models we have so far discussed and several others. Let us consider the torque vector orientation with respect to the magnetic moment of the NS. Because of the symmetry, the alignment torque should vanish for the aligned case, $\alpha = 0^\circ$. The net torque therefore is purely due to the spin-down torque:

it is directed along $-z$ direction and parallel to $\vec{\mu}$.³ Therefore, in projections along $\vec{\mu}$ and perpendicular to $\vec{\mu}$, the torque components become:

$$\alpha = 0^\circ: K_{\parallel} = -A, \quad (18a)$$

$$K_{\perp} = 0, \quad (18b)$$

where $A > 0$ is a number and K_{\parallel} and K_{\perp} are torque components parallel and perpendicular to $\vec{\mu}$, respectively, in the $\vec{\mu}$ – $\vec{\Omega}$ plane. Let us consider an orthogonal rotator, $\alpha = 90^\circ$. Clearly, due to the symmetry of the orthogonal rotator relative to $z = 0$ plane, its alignment torque also vanishes. Therefore the net torque is again purely due to the spin-down torque and points in the $-z$ direction. However, this time this direction is perpendicular to $\vec{\mu}$, therefore:

$$\alpha = 90^\circ: K_{\parallel} = 0, \quad (19a)$$

$$K_{\perp} = -B, \quad (19b)$$

where $B > 0$ is a number. Clearly, a simple dependence on α that satisfies the limiting cases (18) and (19) is

$$\text{Any } \alpha: K_{\parallel} = -A \cos \alpha, \quad (20a)$$

$$K_{\perp} = -B \sin \alpha. \quad (20b)$$

So far we neglected any obliquity-angle dependence of coefficients A and B . This is a good approximation in the simplest cases. For example, for vacuum pulsars the magnetospheric torque is always perpendicular to the magnetic moment, with

$$\text{Vacuum: } A = 0, \quad (21)$$

$$B = 2K_{\text{aligned}}/3. \quad (22)$$

In general, however, coefficients A and B can show some obliquity angle dependence that is specific to an underlying magnetosphere model, so from now on we will implicitly assume that $A = A(\alpha)$, $B = B(\alpha)$.

A simple coordinate transformation gives us (see also Fig. 1)

$$K_x = K_{\parallel} \sin \alpha - K_{\perp} \cos \alpha \quad (23)$$

$$K_z = K_{\parallel} \cos \alpha + K_{\perp} \sin \alpha. \quad (24)$$

Substituting for K_{\parallel} and K_{\perp} according to equations (20), we find

$$K_x = (B - A) \sin \alpha \cos \alpha, \quad (25)$$

$$K_z = -A \cos^2 \alpha - B \sin^2 \alpha, \quad (26)$$

where, according to eqs. (18) and (19), $A|_{\alpha=0^\circ} = -K_z|_{\alpha=0^\circ}$ and $B|_{\alpha=90^\circ} = -K_x|_{\alpha=90^\circ}$ give the spin-down torque for aligned and orthogonal rotators, respectively. Using eqs. (14)–(15), for our MHD model we find that

$$\text{MHD: } A = K_{\text{aligned}} [k_0 + (k_1 - k_2) \sin^2 \alpha], \quad (27)$$

$$B = K_{\text{aligned}} [k_0 + k_2 + (k_1 - k_2) \sin^2 \alpha]. \quad (28)$$

Note that since we approximately have $k_1 \approx k_2$, the coefficients A and B for the MHD pulsar magnetosphere are approximately independent of α , just like in the case of the vacuum pulsar discussed above.

Is there any relationship between the processes of alignment and spindown of the star? If coefficients A and B are independent of obliquity angle α (this is the case for vacuum pulsars and for MHD

³ We note that for simplicity in this section we do not consider the precession torque that does not change the obliquity angle and pulsar rotation rate.

pulsars if $k_1 \approx k_2$), the alignment and spindown torque components are related as

$$K_x = (B - A) \sin \alpha \cos \alpha \equiv [K_z(0^\circ) - K_z(90^\circ)] \sin \alpha \cos \alpha. \quad (29)$$

Since $d\alpha/dt \propto -K_x$ (see §3), and K_z is a monotonic function of the obliquity angle, this relation shows that for any A and B we have:

$$\frac{d\alpha}{dt} \propto \frac{dK_z}{d\alpha} \propto -\frac{d}{d\alpha} \left| I \frac{d\Omega}{dt} \right|, \quad (30)$$

so the pulsar obliquity angle evolves in a way to reduce pulsar spindown losses. Since in both vacuum and MHD scenarios we have $A < B$, pulsar obliquity angle evolves toward zero (aligned pulsar). In the special case, $A = B$, the spindown losses are independent of the obliquity angle. In this case, α does not evolve in time. This is the case of the force-free split-monopole solution discussed in Bogovalov (1999). Finally, if we had $A > B$, the pulsar would have evolved toward $\alpha = 90^\circ$ (orthogonal pulsar). This result was found by Beskin et al. (1993) and is sensitive to their *assumption* about the magnitude of the magnetospheric current, a crucial yet unknown quantity at the time of their work. The advent of force-free (Spitkovsky 2006) and MHD (Tchekhovskoy et al. 2013) magnetospheric models for oblique pulsar magnetospheres demonstrated that the magnitude of the magnetospheric current is substantially different from that assumed by Beskin et al. (1993) (see Appendix A for more detail).

7 DISCUSSION AND CONCLUSIONS

It is well-understood that pulsar magnetospheres are filled with plasma that produces the observed radio through gamma-ray emission. In this paper, we for the first time use self-consistent plasma-filled solutions of pulsar magnetospheres to study the time evolution of pulsar obliquity angle, α . For a spherically-symmetric NS embedded with a magnetic dipole moment, we show that general symmetry considerations require that pulsar obliquity angle evolves such as to minimize pulsar spindown luminosity. Specializing to plasma-filled (force-free or MHD) pulsars, we obtain the expressions for magnetospheric spindown and alignment torques and provide the first self-consistent scenario for the time evolution of the pulsar obliquity angle. We find that plasma-filled pulsars approach alignment as a power-law in time, whereas vacuum pulsars approach alignment exponentially fast. We demonstrate that the cause for the exponential decay in α is the zero spindown luminosity of aligned vacuum pulsars that results in the freeze-out of the pulsar rotational period (see the end of §5 for a discussion).

In this paper we assumed that the NS is spherically symmetric. More detailed calculations that account for non-sphericity of the NS need to be carried out in the case of plasma-filled magnetospheres. Such calculations are presently intrinsically uncertain due to the lack of a detailed understanding of the structure of NS crust and its elastic response. In this light, it is encouraging that the MHD evolution of pulsar obliquity angle in time does not obviously contradict any of the observables. In fact, it naturally explains the production of normal pulsars (with periods of order of one second). This is in contrast to the vacuum pulsar scenario in which, absent stellar non-sphericity, the production of normal pulsars is not possible due to the exponential decay of the obliquity angle that causes the freeze-out of pulsar period (Goldreich 1970; Melatos 2000).

The quantitative treatment of spin-down and obliquity angle evolution is of great importance for pulsar population synthesis studies. It was previously shown that the observed fraction of nearly

orthogonal rotators, which show radio interpulses, cannot be reproduced without accounting for obliquity angle evolution (see, e.g., Weltevrede & Johnston 2008). Our plasma-filled model may self-consistently resolve this issue.

Until now, most of the work in the area of radiopulsar population synthesis has been performed under assumption of magnetodipole losses (see Popov & Prokhorov 2007 for review, see also Faucher-Giguère & Kaspi 2006 and Ridley & Lorimer 2010). The self-consistent physically-motivated plasma-filled model presented in this work can be used to construct more realistic pulsar population synthesis models.

Since our computational star is much larger than the real pulsar, we study for the first time how magnetospheric torques depend on the relative size of the star compared to the size of the light cylinder. We find that smaller stars lose their energy slightly more efficiently. The origin of this dependence will be addressed elsewhere.

In this work we neglected stellar multipole magnetic moments higher than the dipole moment. While this is expected to be a good approximation due to the rapid decay of higher order magnetic moments with radius, the residual contribution of higher-order multipoles at the distances of light cylinder can affect the magnetospheric torques. Importantly, since the alignment torque is set at the surface of the star, its value might be particularly sensitive to the higher order multipole contribution. The effect of multipolar magnetic field configuration on pulsar evolution will be studied in future work.

ACKNOWLEDGEMENTS

We thank A. Spitkovsky, V.S. Beskin, C.-A. Faucher-Giguère, and L. Arzamasskiy for insightful discussions. AT was supported by a Princeton Center for Theoretical Science Fellowship and by NASA through the Einstein Fellowship Program, grant PF3-140115. The simulations presented in this article used computational resources supported by the PICSiE-OIT High Performance Computing Center and Visualization Laboratory, and by XSEDE allocation TG-AST100040 on NICS Kraken and Nautilus and TACC Lonestar, Longhorn and Ranch.

APPENDIX A: MAGNITUDE OF MAGNETOSPHERIC CURRENT AND EVOLUTION OF PULSAR OBLIQUITY ANGLE

In this paper, in order to compute the magnetospheric torques on the NS, we first calculate fluxes of various components of angular momentum. Then, by evaluating those components at the surface of the star, we compute the torque components according to eqs. (2). An alternative approach, used by, e.g., Beskin et al. (1993), is to calculate the torque associated with the Lorentz force arising from the interaction of the NS poloidal field with the surface currents (these currents close the longitudinal currents flowing in the region of open magnetosphere). One can prove by straightforward but cumbersome calculation that the two approaches are identical.

As we explained in §6, Beskin et al. (1993) conclude that pulsar obliquity angle evolves in time toward an orthogonal configuration, which is the opposite of our findings (§6). What is the origin of this discrepancy? A major difference of our work and theirs is that in the absence of a global plasma-filled magnetospheric solution at the time Beskin et al. (1993) *assumed* that the magne-

tospheric current approximately equals the Goldreich-Julian (GJ) current, $j \approx j_{\text{GJ}} = \rho_{\text{GJ}} c$, for all values of obliquity, where ρ_{GJ} is the charge density, which is required to screen the electric field component parallel to the magnetic field and is called Goldreich-Julian charge density (Goldreich & Julian 1969). This is a crucial assumption because pulsar spindown luminosity is proportional to the magnetospheric current squared. Since j_{GJ} is much smaller for an orthogonal rotator than for an aligned rotator, within Beskin et al. (1993) assumption the energy losses are also much smaller for the orthogonal rotator, leading to pulsar obliquity angle evolution towards the orthogonal configuration (see §6).

While for an aligned rotator the assumption of Beskin et al. (1993) was proven accurate, for an orthogonal rotator an ideal plasma-filled (e.g., ideal force-free or MHD) magnetospheric structure requires a much larger current, $j \gg j_{\text{GJ}}$. Thus, the spindown energy losses of a plasma-filled orthogonal rotator are much larger than for a plasma-filled aligned rotator. As discussed in §6, the obliquity angle of a pulsar evolves so as to minimize the spindown energy losses. Therefore, in this case the pulsar evolves in time toward an aligned configuration. Recent simulations of pair production in the inner gap (Timokhin & Arons 2013) suggest that the microphysics of the cascade near the polar cap can support the large currents required by the global magnetospheric structure.

REFERENCES

- Bai X.-N., Spitkovsky A., 2010a, *ApJ*, 715, 1282
 Bai X.-N., Spitkovsky A., 2010b, *ApJ*, 715, 1270
 Beskin V. S., Gurevich A. V., Istomin Y. N., 1993, *Physics of the pulsar magnetosphere*. Cambridge University Press
 Beskin V. S., Philippov A. A., 2012, *MNRAS*, 425, 814
 Bogovalov S. V., 1999, *A&A*, 349, 1017
 Contopoulos I., Kazanas D., Fendt C., 1999, *ApJ*, 511, 351
 Davis L., Goldstein M., 1970, *ApJ*, 159, L81
 Deutsch A. J., 1955, *Annales d'Astrophysique*, 18, 1
 Faucher-Giguère C.-A., Kaspi V. M., 2006, *ApJ*, 643, 332
 Gammie C. F., McKinney J. C., Tóth G., 2003, *ApJ*, 589, 444
 Goldreich P., 1970, *ApJ*, 160, L11
 Goldreich P., Julian W. H., 1969, *ApJ*, 157, 869
 Gruzinov A., 2005, *Physical Review Letters*, 94, 021101
 Kalapotharakos C., Contopoulos I., 2009, *A&A*, 496, 495
 Kalapotharakos C., Contopoulos I., Kazanas D., 2012, *MNRAS*, 420, 2793
 Komissarov S. S., 2006, *MNRAS*, 367, 19
 Landau L. D., Lifshitz E. M., 1960, *Electrodynamics of continuous media*. Pergamon Press
 Li J., Spitkovsky A., Tchekhovskoy A., 2012, *ApJ*, 746, 60
 Lyne A. G., Graham-Smith F., 1998, *Pulsar astronomy*
 Lyubarsky Y., 2008, in Bassa C., Wang Z., Cumming A., Kaspi V. M., eds, *40 Years of Pulsars: Millisecond Pulsars, Magnetars and More* Vol. 983 of American Institute of Physics Conference Series, Pulsar emission mechanisms. pp 29–37
 McKinney J. C., 2006, *MNRAS*, 368, L30
 McKinney J. C., Blandford R. D., 2009, *MNRAS*, 394, L126
 McKinney J. C., Tchekhovskoy A., Blandford R. D., 2012, *MNRAS*, 423, 3083
 Melatos A., 2000, *MNRAS*, 313, 217
 Michel F. C., Goldwire Jr. H. C., 1970, *Astrophys. Lett.*, 5, 21
 Pétri J., 2012, *MNRAS*, 424, 605
 Popov S. B., Prokhorov M. E., 2007, *Soviet Physics Uspekhi*, 50, 1123
 Ridley J. P., Lorimer D. R., 2010, *MNRAS*, 404, 1081
 Spitkovsky A., 2006, *ApJ*, 648, L51
 Tchekhovskoy A., McKinney J. C., Narayan R., 2007, *MNRAS*, 379, 469
 Tchekhovskoy A., Narayan R., McKinney J. C., 2011, *MNRAS*, 418, L79
 Tchekhovskoy A., Spitkovsky A., Li J., 2013, *ArXiv:1211.2803*
 Timokhin A. N., 2006, *MNRAS*, 368, 1055
 Timokhin A. N., Arons J., 2013, *MNRAS*, 429, 20
 Weltevrede P., Johnston S., 2008, *MNRAS*, 387, 1755